Inorganic Chemistry

Article

pubs.acs.org/IC

Rhodamine-Based Fluorescent Probe for Al^{3+} through Time-Dependent PET–CHEF–FRET Processes and Its Cell Staining Application

Animesh Sahana,[†] Arnab Banerjee,[†] Sisir Lohar,[†] Bidisha Sarkar,[‡] Subhra Kanti Mukhopadhyay,[‡] and Debasis Das*[,†]

[†]Department of Chemistry and [‡]Department of Microbiology, The University of Burdwan, Burdwan 713104, West Bengal, India

Supporting Information

ABSTRACT: Rhodamine-diformyl *p*-cresol conjugate (L) has been developed as a novel Al^{3+}-selective fluorometric and colorimetric sensor based on the FRET mechanism for the first time. L can selectively detect Al^{3+} through time-dependent PET–CHEF and FRET processes. This phenomenon is nicely reflected from ^1H NMR, fluorescence lifetime, and fluorescence cell imaging studies. The probe can detect Al^{3+} as low as 5×10^{-9} M in HEPES-buffered EtOH:water (0.1 M, 4:1, v/v, pH 7.4). The probe shows pH-dependent emission properties viz. an intense red emission (585 nm) at acidic pH and an intense green fluorescence (535 nm) at basic pH. Thus, L can also be used as a pH sensor via tunable wavelength.

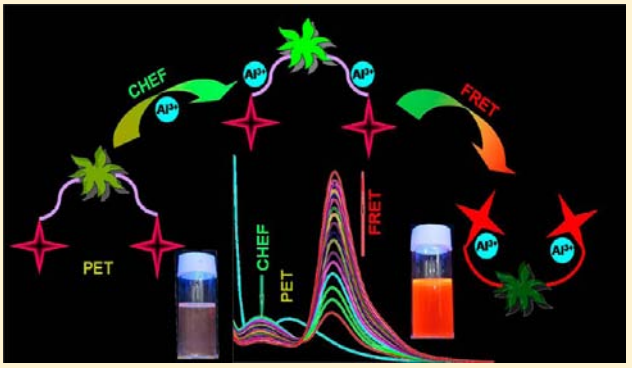

INTRODUCTION

Aluminum, a nonessential element, is a competitive inhibitor in different biological processes involving several essential elements viz. Mg^{2+} (0.066 nm), Ca^{2+} (0.099 nm), and Fe^{3+} (0.064 nm) due to its similarities regarding atomic size (0.051 nm) and charge (3+). Acid rain increases the concentration of Al^{3+} in soil, which is deadly to living plants.[1,2] Al^{3+} toxicity causes microcytic hypochromic anemia, Al-related bone disease (ARBD), encephalopathy, neuronal disorder leading to dementia, myopathy, and Alzheimer's disease.[3] The WHO recommended the average daily human intake of Al^{3+} of around 3–10 mg and weekly tolerable dietary intake as 7 mg kg^{-1} body weight.[4] Thus, trace level determination of Al^{3+} is highly important.

Among several methods[5] for determination of Al^{3+}, the fluorescence method has become very popular due to its useful applications in environmental chemistry, medicine, and biology.[6] The poor coordination ability of Al^{3+} has hindered development of a suitable fluorescence sensor.[7] However, recently, the design and synthesis of Al^{3+}-selective fluorescent probes has received considerable attention.[8]

Design of a fluorescent probe is generally based on intramolecular charge transfer (ICT),[9] photoinduced electron transfer (PET),[10] chelation-enhanced fluorescence (CHEF),[11] metal–ligand charge transfer (MLCT),[12] excimer/exciplex formation,[13] imine isomerization,[14] intermolecular hydrogen bonding,[15] excited-state intramolecular proton transfer,[16] displacement approach,[17] and fluorescence resonance energy transfer.[18] FRET is currently an active research area due to its practical application in cell physiology, optical therapy, and selective sensing of ionic species.[19] FRET is an excited-state interaction between two fluorophores where excitation energy from the donor (D) is transferred to a nearby energy acceptor (A) via long-range dipole–dipole interaction and/or short-range multipolar interaction. Thus, FRET is associated with a certain degree of overlap between the fluorescence emission spectrum of the donor (D) and the absorbance spectrum of the acceptor (A). A FRET-based fluorescent probe generally demands an appropriate energy donor (D), an energy acceptor (A), and a suitable linker to connect them. It is well known that spirocyclic rhodamine derivatives are a useful platform for selective sensing of ionic species leading to spirolactam ring opening.[20,21]

EXPERIMENTAL SECTION

General Procedures. High-purity HEPES, rhodamine B, *p*-cresol, and ethylenediamine were purchased from Sigma Aldrich (India). $Al(NO_3)_3 \cdot 9H_2O$ was purchased from Merck (India). Solvents used were spectroscopic grade. *N*-(Rhodamine-B)lactam-ethylenediamine was prepared according to the literature method.[22] 2,6-Diformyl-4-methylphenol was prepared by modification of the literature method.[23] All metal salts were used as either their nitrate or their chloride salts. Other chemicals were of analytical reagent grade and used without further purification except when specified. Milli-Q Milipore 18.2 MΩ cm^{-1} water was used throughout all experiments. A JASCO (model V-570) uv–vis spectrophotometer was used for recording UV–vis spectra. FTIR spectra were recorded on a JASCO FTIR spectrophotometer (model FTIR-H20). Mass spectra were carried out using a

Received: September 13, 2012
Published: March 13, 2013

   dx.doi.org/10.1021/ic3019953 | *Inorg. Chem.* 2013, 52, 3627–3633

Scheme 1. Syntheses of L and L1

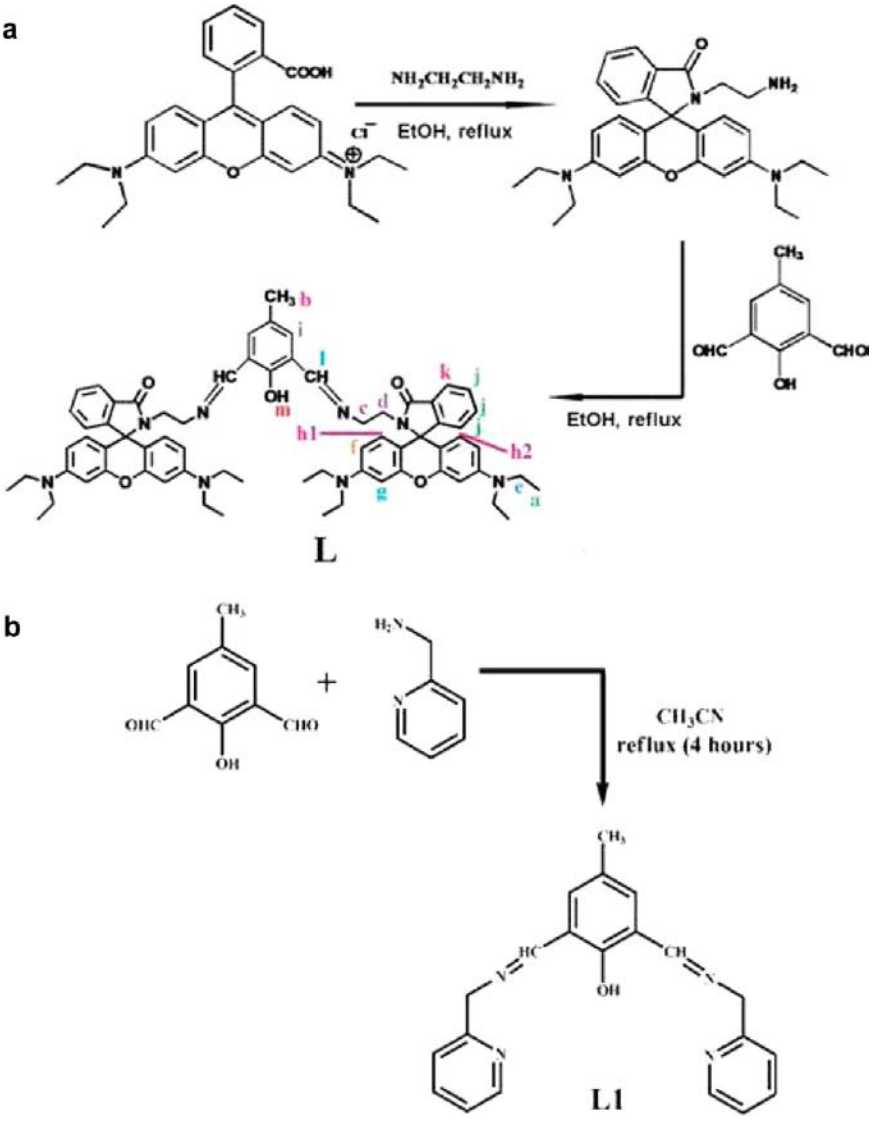

QTOF Micro YA 263 mass spectrometer in ES positive mode. ^{1}H NMR spectra were recorded using a Bruker Avance 600 (600 MHz) in DMSO-d_6 and Bruker Avance 500 (500 MHz) in $CDCl_3$, whereas ^{13}C NMR spectra were recorded using a Bruker Avance 300 (75 MHz) in CD_3OD. Melting point was measured with a VEEGO digital melting point apparatus. Elemental analysis was performed using a Perkin-Elmer CHN-Analyzer with the first 2000-Analysis kit. Steady-state fluorescence emission and excitation spectra were recorded with a Hitachi F-4500 spectrofluorometer. A Systronics digital pH meter (model 335) was used to measure the solution pH. Either 50 mM HCl or KOH was used for pH adjustment. Time-resolved fluorescence lifetime measurements were performed using a picosecond pulsed diode laser-based time-correlated single-photon counting (TCSPC) spectrometer from IBH (UK) at λ_{ex} 470 nm and MCP-PMT as a detector. Emission from the sample was collected at a right angle to the direction of the excitation beam maintaining magic angle polarization (54.71).The full width at half-maximum (fwhm) of the instrument response function was 250 ps, and the resolution was 28 ps per channel. Data were fitted to multiexponential functions after deconvolution of the instrument response function by an iterative reconvolution technique using IBH DAS 6.2 data analysis software in which reduced w2 and weighted residuals serve as parameters for goodness of fit.

Imaging System. The imaging system was composed of an inverted fluorescence microscope (Leica DM 1000 LED), a digital compact camera (Leica DFC 420C), and an image processor (Leica Application Suite v3.3.0). The microscope was equipped with a mercury 50 W lamp.

Preparation of Cells. Pollen grains were collected from fresh mature buds of *Allamanda puberula* (Aapocynaceae), a common ornamental plant with a bell-shaped bright yellow flower by crashing stamens on a sterile petriplate and suspending them in normal saline. After crashing the stamina debrishes were removed by filtering through a thin layer of nonabsorbant cotton and the suspended pollens were collected by centrifugation at 5000 rpm for 5 min. The pollen pellet was then washed twice in normal saline and incubated in a solution of $Al(NO_3)_3{\cdot}9H_2O$ (0.1 mg/mL) for 1 h at ambient temperature. After incubation, they were again washed in normal saline and photographed under a fluorescence microscope in the presence and absence of **L**. Both Al^{3+}-treated and untreated cells were stained with **L** and observed under a fluorescence microscope.

Synthesis of L. A portion of *N*-(rhodamine-B)lactam-ethylenediamine (1 g, 2.06 mmol) and diformyl *p*-cresol (0.167 g, 1.030 mmol) was combined in fresh distilled ethanol (30 mL). The reaction mixture was refluxed for 24 h and stirred for another 2 h at room temperature to form an orange precipitate. Solid was filtrated and washed with ethanol three times. Crude product was purified by recrystallization from acetonitrile to give 1.036 g of **L** (orange solid) in 89% yield; MP 245 °C (±4 °C). ^{1}H NMR (600 MHz, DMSO-d_6) (Figure S1, Supporting Information): 1.09 (24H, m, J = 7.2 Hz, a); 2.19 (3H, s,

dx.doi.org/10.1021/ic3019953 | *Inorg. Chem.* 2013, 52, 3627−3633

b); 2.53 (4H, s, c); 2.97 (4H, m, J = 7.2 Hz, d); 3.25 (16H, m, J = 7.8 Hz, e); 6.32 (4H, d, J = 8.4 Hz, f); 6.36 (4H, d, J = 7.8 Hz, g); 6.99 (2H, d, J = 15.6 Hz, h1); 7.03 (2H, d, J = 4.8 Hz, h2); 7.33 (2H, s, i); 7.52−7.46 (6H, m, J = 6 Hz, j); 7.78 (2H, m, J = 4.8 Hz, k); 8.12 (2H, s, l). ^{13}C NMR (75 MHz, CD_3OD) (Figure S2, Supporting Information): δ 170.64, 155.23, 155.04, 154.96, 150.60, 150.52, 134.34, 132.26, 129.95, 129.73, 125.31, 123.73, 109.76, 106.38, 106.31, 99.17, 67.20, 45.54, 44.13, 41.24, 40.61, 20.57, 13.16, 13.05. QTOF-MS ES$^+$ (Figure S3, Supporting Information): $[M + H]^+$ = 1097.24; $[M + Na]^+$ = 1119.19. Anal. Calcd for $C_{69}H_{76}N_8O_5$: C, 75.52; H, 6.98; N, 10.21. Found: C, 75.47; H, 6.91; N, 10.24. FTIR/cm^{-1} (Figure S4, Supporting Information): υ(OH) 3428.07, υ(C═O) 1686.35, υ(C═N) 1630.76.

Synthesis of L1. To a solution of 2-picolyl amine (0.133 g, 1.23 mmol) in acetonitrile (10 mL), 10 mL of an acetonitrile solution of diformyl *p*-cresol (0.100 g, 0.617 mmol) was added dropwise. The reaction mixture was refluxed for 4 h to form a yellow precipitate. Solid was filtered and washed with ethanol three times. Crude product was purified by recrystallization from acetonitrile to give 0.193 g of **L1** (yellow solid) in 82.8% yield; MP 143 °C (±4 °C). ^{1}H NMR (500 MHz, $CDCl_3$) (Figure S5, Supporting Information), 2.03 (3H, s, a); 4.99 (4H, m, J = 10.0 Hz, b); 7.73−7.12 (10H, m, J = 10.0 Hz, c); 8.55 (2H, s, d). QTOF-MS ES$^+$ (Figure S6, Supporting Information): $[M + H]^+$ = 345.08; $[M + Na]^+$ = 367.08. Anal. Calcd for $C_{21}H_{20}N_4O$: C, 73.23; H, 5.85; N, 16.27. Found: C, 73.11; H, 5.89; N, 16.21. FTIR/cm^{-1} (Figure S7, Supporting Information): υ(OH) 3376.28, υ(C═N) 1637.62.

Synthesis of L−Al^{3+} Complex. To 2 mL of a solution of $Al(NO_3)\cdot 9H_2O$ (0.17 g, 0.0456 mmol) in water, an ethanol solution of **L** (0.25 g, 0.0228 mmol, 8 mL) was added dropwise and stirred for 5 min. Solvent was removed using a rotary evaporator, while a blood red precipitate was obtained. QTOF-MS ES$^+$ (Figure S8, Supporting Information): $[M + H]^+$ = 1615.14. FTIR/cm^{-1} (Figure S9, Supporting Information): υ(C═O) 1642.67, υ(C═N) 1626.79, $\upsilon(NO_3^-)$ 1383.50.

RESULTS AND DISCUSSION

DFP-rhodamine (DFP = 2, 6-diformyl-4-methylphenol) conjugate (**L**) is established as a FRET "off−on" system for selective intracellular Al^{3+} sensing. Al^{3+} efficiently induces ring opening of the rhodamine unit, which acts as an energy acceptor. DFP is chosen as the energy donor due to its intense fluorescence spectrum which overlaps with the absorption spectrum of the rhodamine B unit (Figure S10, Supporting Information). Scheme 1a shows the synthesis of **L**. In the presence of Al^{3+}, the emission maxima of **L** shifts from 535 (characteristic of DFP, PET) to 585 nm (characteristic of rhodamine B, FRET) via an intermediate CHEF process with a characteristic emission band at 509 nm. Very weak emission of **L** at 535 nm may be due to the PET process from the N-donor site of the spirolactam ring to the DFP moiety. To establish the above stated fact, a model compound (**L1**) has been synthesized (Scheme 1b) and characterized. In the model compound **L1**, the acceptor part (rhodamine unit) is replaced by a 2-picolyl amine moiety. Upon excitation at 400 nm, **L1** emits at 500 nm in HEPES-buffered EtOH:water (0.1 M, 4:1, v/v, pH 7.4), attributed to the PET from the N center of the pyridyl moiety to DFP. In the presence of Al^{3+}, the emission maximum of **L1** is blue shifted to 460 nm due to CHEF (Figure S11, Supporting Information). The absence of an emission band at 585 nm in **L1** suggests the absence of a FRET process. Hence, emission at 585 nm in **L** is ascribed to the Al^{3+}-induced FRET process. Moreover, the absence of an absorbance at 555 nm in **L1** supports the absence of a FRET process (Figure S12, Supporting Information). To confirm the CHEF process, **L**−Al^{3+} complex is isolated and characterized by mass and FTIR spectra (Figures S8 and S9, Supporting Information). To the best of our knowledge, this is the first report on rhodamine B-based Al^{3+} sensor where all interaction steps viz. PET−CHEF−FRET have been observed distinctly as a function of time and been reflected in time-dependent living cell imaging.

The photophysical properties of **L** have been studied in HEPES-buffered EtOH:water (0.1 M, 4:1, v/v, pH 7.4). **L** (10 μM) shows a yellow-green emission band centered at 535 nm (λ_{ex} = 460 nm) which is attributed to the PET process with a quantum yield of 4.6 × 10^{-2} at room temperature. No FRET is observed in free **L** due to the presence of a spirolactam ring in the rhodamine B unit. After 1 min of addition of Al^{3+} (30 μM) to **L** (10 μM), two emission bands centered at 509 and 585 nm are observed (Figure 1).[24] The emission band at 509 nm (green

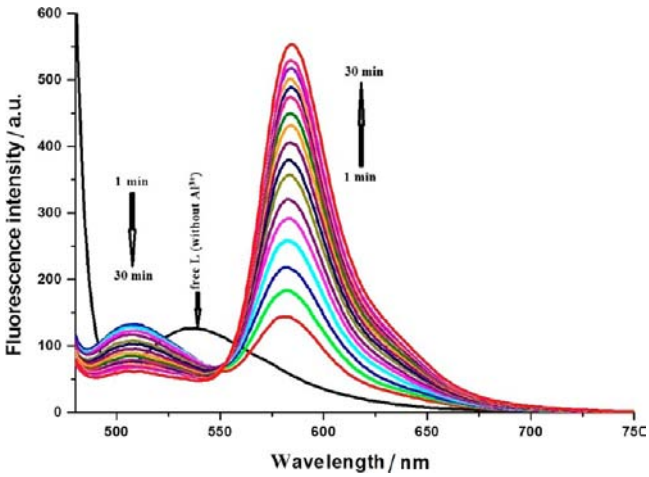

Figure 1. Variation of the fluorescence intensity of **L** (10 μM) in the presence of Al^{3+} (30 μM) in HEPES-buffered (0.1 M) EtOH:water (4:1, v/v), pH 7.4 with time (λ_{ex} = 460 nm).

fluorescence) is due to the intermediate CHEF process, whereas the band at 585 nm (red fluorescence) is ascribable to the Al^{3+}-induced FRET process. After 30 min, the emission band at 509 nm diminishes with the appearance of an intense emission band at 585 nm (Figure S13, Supporting Information), due to the spirolactam ring opening of rhodamine unit. Addition of Al^{3+} (30 μM) to **L** (10 μM) increases the fluorescence quantum yield 6.9 times (31.7 × 10^{-2}). Time-dependent color changes of the **L**−Al^{3+} system under a hand-held UV lamp are presented in Figure 2. Detection of an intermediate CHEF process has become possible due to the slow interaction kinetics between **L** and Al^{3+}. The pseudo-first-order rate constant has been estimated as 0.0871 min^{-1} by measuring the changes in the fluorescence intensity at 585 nm (Figure S14, Supporting Information). Fluorescence titration of **L** (10 μM) with Al^{3+} in HEPES-buffered EtOH:water (0.1 M, 4:1, v/v, pH 7.4) revealed that the emission intensity at 509 and 585 nm increases with increasing Al^{3+} concentration (Figure 3). A plot of emission intensity (at 585 nm) vs concentration of Al^{3+} is linear up to 50 μM (Figure S15, Supporting Information).[25] Figure S16, Supporting Information, shows the fluorescence titration at 509 nm, which is attributed to the CHEF process. Interestingly, the plot of emission intensity vs concentration of Al^{3+} (at 509 nm) is linear up to 40 μM (Figure S17, Supporting Information). Emission at 585 nm (λ_{ex} = 525 nm) is attributed to the open ring spirolactam form of the rhodamine B

dx.doi.org/10.1021/ic3019953 | Inorg. Chem. 2013, 52, 3627−3633

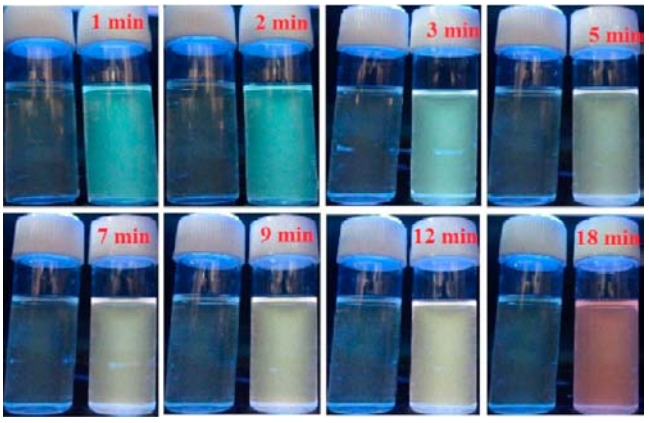

Figure 2. Al^{3+}-induced color changes of **L** in EtOH:water (4:1, v/v) as a function of time observed under a hand-held UV lamp.

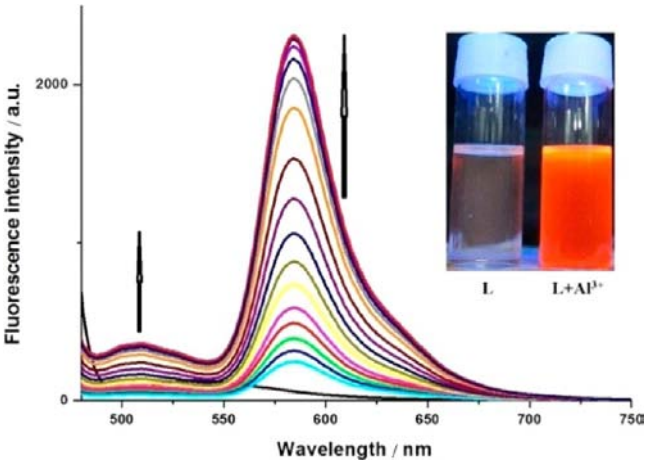

Figure 3. Fluorescence spectra of **L** (10 μM) in HEPES-buffered (0.1 M) EtOH:water (4:1, v/v, pH 7.4) upon addition of increasing amounts of Al^{3+} (0, 10, 15, 20, 25, 30, 35, 40, 45, 50, 55, 60, 65, 70, 75, 80, 85, 90 μM) (λ_{ex} = 460 nm). (Inset) Distinct color change of **L** upon addition of Al^{3+}. All spectra are recorded after 40 min of mixing of Al^{3+} and **L**.

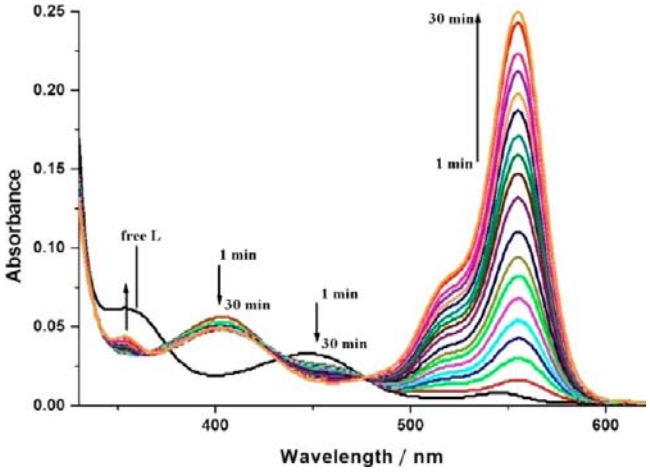

Figure 4. Variation of the absorbance of **L** (10 μM) as a function of time in the presence of Al^{3+} (60 μM) in HEPES buffer (0.1 M) (EtOH:water, 4:1, v/v, pH 7.4).

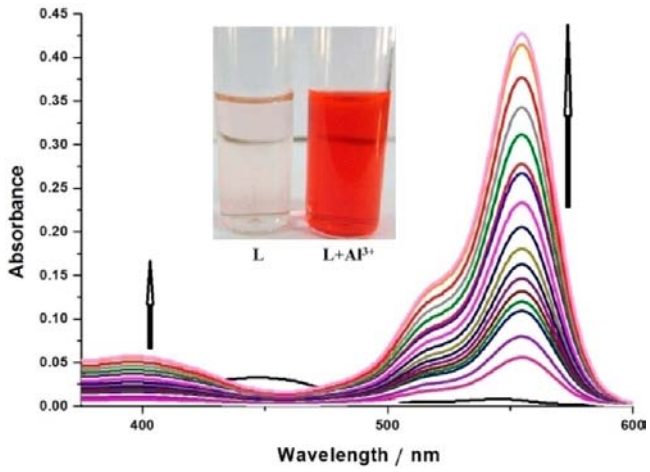

Figure 5. Changes in the absorption spectra of **L** (10 μM) in HEPES-buffered (0.1 M, EtOH:water, 4:1, v/v, pH 7.4) upon gradual addition of Al^{3+} (0, 10, 15, 20, 25, 30, 35, 40, 45, 50, 55, 60, 65, 70, 75, 80, 85, 90 μM). (Inset) Distinct color change of **L** upon addition of Al^{3+}. All spectra are recorded after 40 min of mixing of Al^{3+} and **L**.

derivative, the intensity of which gradually increases with increasing Al^{3+} concentration (Figure S18, Supporting Information). **L** (10 μM) shows absorbance centered at 460 nm. Addition of Al^{3+} (60 μM) to the colorless solution of **L** (10 μM) results in an intense red color solution due to spirolactam ring opening of the rhodamine B unit. After 1 min, two new bands appear at 400 and 555 nm (Figure 4), indicating **L**–Al^{3+} complex formation and Al^{3+}-induced spirolactam ring-opening processes, respectively. Moreover, absorbance at 400 nm decreases with time, while it increases at 555 nm. Gradual addition of Al^{3+} to the solution of **L** (10 μM) increases absorbance at two different wavelengths viz. 400 and 555 nm (Figure 5) along with distinct color change. A linear plot of absorbance vs Al^{3+} concentration (Figure S19, Supporting Information) is useful to determine unknown Al^{3+} concentration. **L** shows excellent selectivity for Al^{3+} as other common cations (Figures S20 and S21, Supporting Information) do not interfere. Hg^{2+} shows slight increase of fluorescence (Figure S22, Supporting Information) in which only FRET but no intermediate CHEF process is observed. Interference from Hg^{2+} is eliminated using KI (Figures S23 and S24, Supporting Information). KI do not interfere with the emission and absorbance of the [**L**–Al^{3+}] system (Figures S25 and S26, Supporting Information). It is found that common metal ions (200 μM) do not interfere in the fluorometric (Figure S27, Supporting Information) and colorimetric (Figure S28, Supporting Information) detection of Al^{3+}. Fluorescence intensity of **L** (0.1 μM) increases with increasing concentration of Al^{3+} (Figure S29, Supporting Information). The plot of emission intensity vs concentration of Al^{3+} is linear from 0.05 to 0.8 μM (Figure S30, Supporting Information). The detection limit of **L** for Al^{3+} is 5×10^{-9} M. Job's plot indicates 2:1 stoichiometry (mole ratio) of the [**L**–Al^{3+}] complex (Figure S31, Supporting Information). The apparent binding constant of **L** for Al^{3+} has been determined using modified the Benesi–Hildebrand[26] equation: $(F_{max} - F_0)/(F_x - F_0) = 1 + (1/K)\,(1/[M]^n)$, where F_{max}, F_0, and F_x are fluorescence intensities of **L** in the presence of Al^{3+} at saturation, free **L**, and any intermediate Al^{3+}concentration. A plot of $(F_{max} - F_0)/(F_x - F_0)$ vs $1/[M]^2$ (here $n = 2$) yields the apparent binding constant value as 9.1×10^6 M^{-2} ($R^2 = 0.995$) (Figure S32, Supporting Information).

dx.doi.org/10.1021/ic3019953 | Inorg. Chem. 2013, 52, 3627–3633

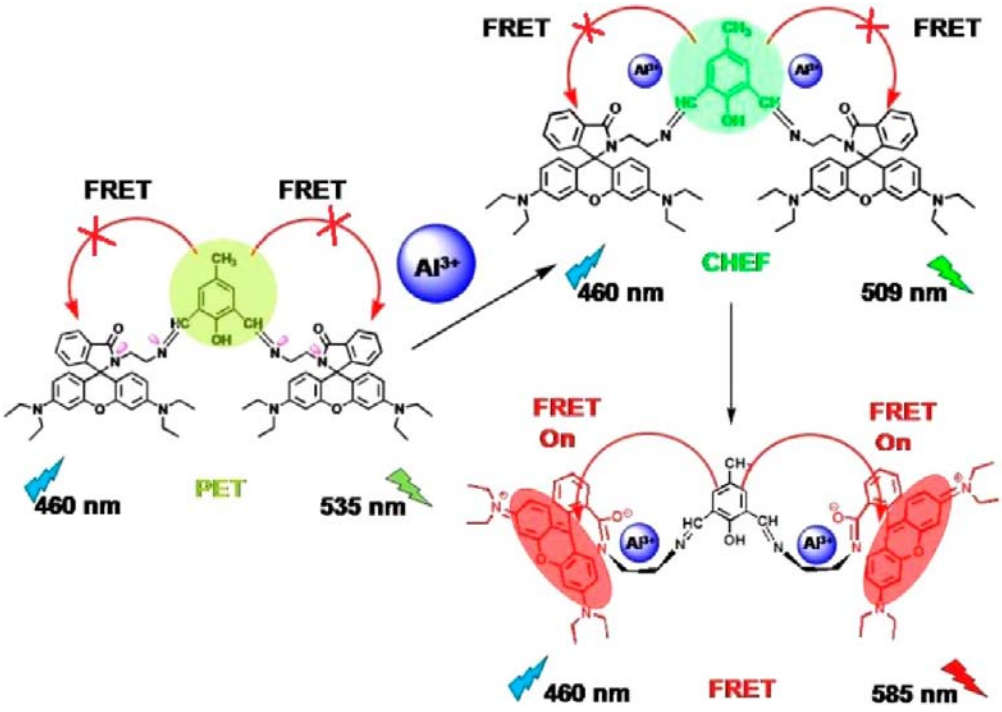

Figure 6. Proposed binding mechanism of **L** to Al^{3+}.

The initial weak fluorescence of **L** may be due to the photoinduced electron transfer (PET) from the N center of the spirolactam ring to the *p*-cresol moiety. Addition of Al^{3+} results in CHEF between **L** and Al^{3+} with inhibition of PET. With increasing time, CHEF emission decreases due to Al^{3+}-induced spirolactam ring opening, leading to FRET (Figure 6). Naked eye detection of Al^{3+} on a paper soaked with **L** is presented in Figure S33, Supporting Information.

The proposed mechanism is well supported by fluorescence lifetime data (Table 1). In the fluorescence lifetime experiment

Table 1. Fluorescence Lifetime Decay Parameters of L and Its Al^{3+} Complex

	B_1	τ_1/ns	B_2	τ_2/ns	$\langle\tau_2\rangle$/ns
L at 535 nm	0.2590	0.141	0.0094	2.506	0.2243
[**L**–Al^{3+}] at 509 nm after 5 min	0.2248	0.145	0.0234	4.350	0.5410
[**L**–Al^{3+}] at 509 nm after 30 min	0.2770	0.115	0.0150	3.870	0.3045
[**L**–Al^{3+}] at 585 nm after 30 min	0.0390	0.418	0.0837	1.730	1.310

(λ_{em} = 535 nm), the average lifetime was found to be 0.2243 ns. After 5 min of addition of Al^{3+} to **L**, the average lifetime (at λ_{em} = 509 nm) of the **L**–Al^{3+} system increased to 0.541 ns, ascribed to the CHEF process. After 30 min, the value reduces to 0.3045 ns. Thus, the CHEF process of the **L**–Al^{3+} system decreases with time as proposed in the mechanism (Figure 7), whereas after 30 min the average lifetime of the **L**–Al^{3+} system at λ_{em} = 585 nm, attributed to the Al^{3+}-induced FRET process, increases to 1.31 ns (Figure 8).

^{1}H NMR Titration. In order to strengthen the above mechanism, ^{1}H NMR titration has been performed by concomitant addition of Al^{3+} to the DMSO-d_6 solution of **L** (Figures S34 and S35, Supporting Information). Significant spectral changes of **L** are observed upon addition of Al^{3+}. After

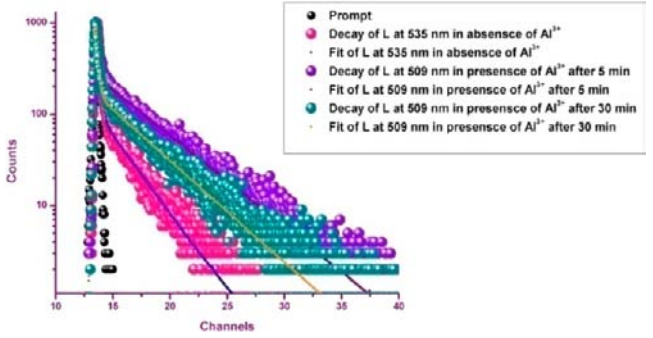

Figure 7. Fluorescence lifetime decay of **L** and the **L** +Al^{3+} system.

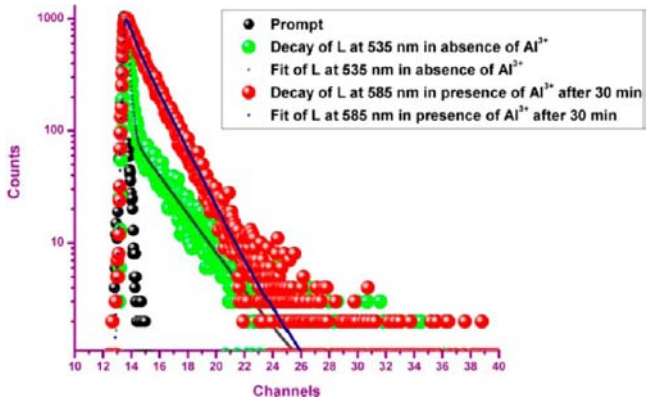

Figure 8. Fluorescence lifetime decay of **L** and the **L** +Al^{3+} system at different wavelengths.

5 min of addition of Al^{3+} to **L**, its **d** protons have been shifted upfield from 2.97 to 2.38 ppm, attributed to Al^{3+}-induced spirolactam ring opening of **L**. After 20 min, **d** protons have been shifted downfield to 2.42 ppm, ascribed to the Al^{3+}-induced FRET process. Additionally, **h1** protons also shifted

dx.doi.org/10.1021/ic3019953 | *Inorg. Chem.* 2013, 52, 3627–3633

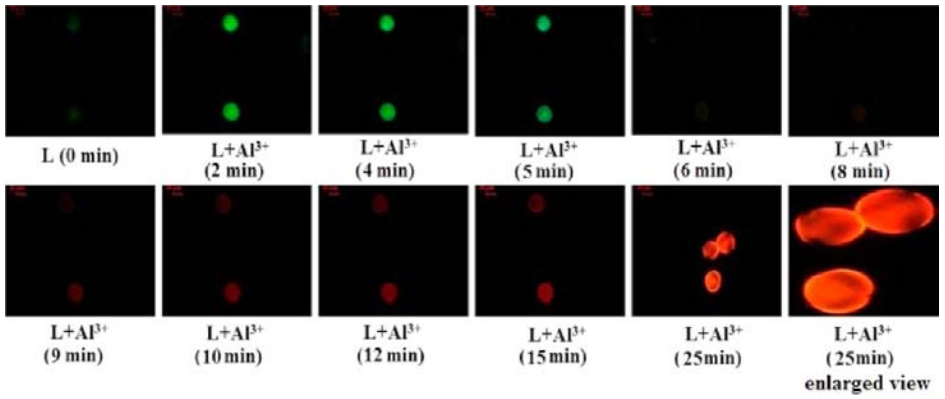

Figure 9. Fluorescence microscopic images of *Allamanda puberula* (Aapocynaceae) cells loaded with **L** (10 μM) as a function of time under a 100× objective lens and **L**-stained cells pre-exposed to 100 μM Al^{3+} for 25 min under a 100× objective lens. Incubation temperature is 37 °C.

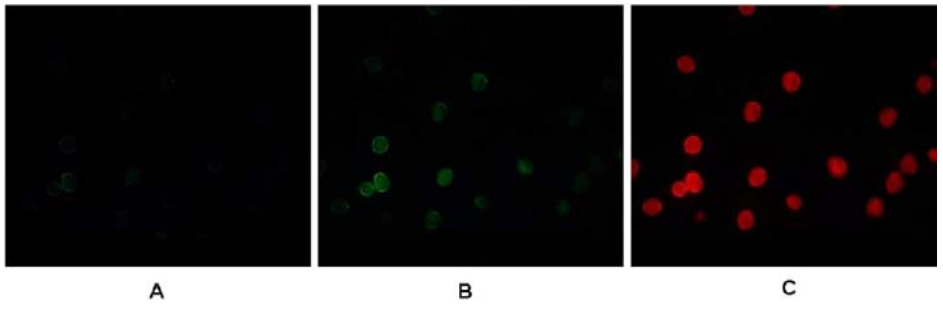

Figure 10. Fluorescence microscopic images of *Allamanda puberula* (Aapocynaceae) cells treated with **L** (10 μM) at (A) pH 7.4, (B) pH 9.0, and (C) pH 5.0. Incubation temperature is 37 °C.

upfield from 6.99 to 6.41 ppm after 5 min of addition of Al^{3+} to **L**. After 20 min of addition of Al^{3+} to **L**, **h1** protons undergo a downfield shift from 6.41 to 6.42 ppm due to the FRET process. After 40 min, **h1** protons move further downfield to 6.45 ppm. Interestingly, after 20 min, **i** protons are partially downfield shifted from 7.33 to 7.58 ppm due to the close proximity of the rhodamine unit during Al^{3+}-induced folding of **L**. After 40 min, **i** protons are completely downfield shifted to 7.6 ppm. **l** protons of **L** have gradually shifted downfield from 8.12 (free **L**) to 8.64 ppm upon interaction with Al^{3+}. All other protons of **L** viz. **a**, **b**, **c**, **e**, **f**, **g**, **h2**, **j**, and **k** have been shifted downfield after interaction with Al^{3+} (Table S1, Supporting Information).

Cell Imaging Studies. Time-dependent living cell imaging studies reveal distinct different colors supporting PET−CHEF−FRET processes. Pollen cells, incubated with Al^{3+} for 30 min, are observed under a fluorescence microscope after adding **L**. Cells are found to emit green fluorescence, the intensity of which decreases with time. After 9 min green fluorescence is changed to red fluorescence, the intensity of which increases with time. Color changes resulting from Al^{3+}-induced time-dependent fluorescence of **L** are presented in Figure 9.

Due to the protonation of the nitrogen center, the spirolactam ring of the rhodamine unit opens at acidic pH[27] along with an intense red emission at 585 nm, whereas at basic pH deprotonation of the −OH group results an intense green fluorescence at 535 nm (Figure S36, Supporting Information). At close to neutral pH (pH 7.4), **L** shows an absorbance maxima at 460 nm. At basic and acidic pH, absorbance maxima move to 435 (green color) and 555 nm (red color), respectively (Figure S37, Supporting Information). Thus, **L** may also be used as pH sensor. pH-dependent emission properties of **L** (10 μM) have also been visualized in living cell imaging. Pollen cells have been incubated with **L** (10 μM) for 30 min. Cells emit very weak green fluorescence at pH 7.4 and become bright green at pH 9.0 and red at pH 5.0 (Figure 10).

CONCLUSION

A novel rhodamine B derivative has been established as an excellent fluorescent and colorimetric probe for Al^{3+}. It can detect Al^{3+} in HEPES-buffered EtOH:water (0.1 M, 4:1, v/v, pH 7.4) as low as 5×10^{-9} M. Selective interaction of **L** with Al^{3+} involves time-dependent PET−CHEF−FRET processes, which has been reflected in living cell imaging under a fluorescence microscope. Additionally, its absorbance and emission can be tuned with pH.

ASSOCIATED CONTENT

Supporting Information

This material is available free of charge via the Internet at http://pubs.acs.org.

AUTHOR INFORMATION

Corresponding Author

*E-mail: ddas100in@yahoo.com.

Notes

The authors declare no competing financial interest.

ACKNOWLEDGMENTS

The authors sincerely thank UGC-DAE-CRS-Kolkata for financial support. A.S. and S.L. are thankful to CSIR, New Delhi, for providing a fellowship. We gratefully acknowledge

Prof. Asok K. Mukherjee for his valuable guidance and inspiration. We sincerely acknowledge the Indian Institute of Chemical Biology (IICB) and University Science Instrumentation Center, Burdwan University, for providing NMR, mass spectra, and fluorescence microscope facilities, respectively. We sincerely thank Prof. Samita Basu and Mr. Ajay Das, Chemical Science Division, SINP, Kolkata, for enabling TCSPC instrument. We gratefully acknowledge Dr. Adinath Majee and Monoranjan Ghosh, Visva-Bharati University, for providing recording some NMR spectra. We are thankful to the learned reviewers for valuable suggestions.

REFERENCES

(1) (a) Delhaize, E.; Ryan, P. R. *Plant Physiol.* **1995**, *107*, 315. (b) Godbold, D. L.; Fritz, E.; Huttermann, A. *Proc. Natl. Acad. Sci. U.S.A.* **1988**, *85*, 3888.

(2) Rout, G. R.; Roy, S. S.; Das, P. *Agronomie* **2001**, *21*, 3.

(3) (a) Gupta, V. K.; Jain, A. K.; Maheshwari, G. *Talanta* **2007**, *72*, 1469. (b) Flaten, T. P. *Brain Res. Bull.* **2001**, *55*, 187.

(4) (a) Barcelo, J.; Poschenrieder, C. *Environ. Exp. Bot.* **2002**, *48*, 75. (b) Valeur, B.; Leray, I. *Coord. Chem. Rev.* **2000**, *205*, 3. (c) Krejpcio, Z.; Wojciak, R. W. P. J. *Environ. Studies* **2002**, *11*, 251.

(5) (a) Ahmad, M.; Narayanaswamy, R. *Talanta* **1995**, *42*, 1337. (b) Saito, S.; Shimidzu, J.-I.; Yoshimoto, K.; Maeda, M.; Aoyama, M. *J. Chromatogr. A* **2007**, *1140*, 230. (c) Murko, S.; Milačič, R.; Ščančar, J. *J. Inorg. Biochem.* **2007**, *101*, 1234. (d) Kralj, B.; čančar, J. Š.; Križaj, I.; Benedik, M.; Bukovec, P.; Milačič, R. *J. Anal. At. Spectrom.* **2004**, *19*, 101.

(6) (a) Quang, D. T.; Kim, J. S. *Chem. Rev.* **2010**, *110*, 6280. (b) Kobayashi, H.; Ogawa, M.; Alford, R.; Choyke, P. L.; Urano, Y. *Chem. Rev.* **2010**, *110*, 2620. (c) Callan, J. F.; de Silva, A. P.; Magri, D. C. *Tetrahedron* **2005**, *61*, 8551. (d) Demchenko, A. P. *Introduction to Fluorescence Sensing*; Springer: New York, 2008.

(7) Soroka, K.; Vithanage, R. S.; Phillips, D. A.; Walker, B.; Dasgupta, P. K. *Anal. Chem.* **1987**, *59*, 629.

(8) (a) Wang, L.; Qin, W.; Tang, X.; Dou, W.; Liu, W.; Teng, Q.; Yao, X. *Org. Biomol. Chem.* **2010**, *8*, 3751. (b) Upadhyay, K. K.; Kumar, A. *Org. Biomol. Chem.* **2010**, *8*, 4892. (c) Hau, F. K.; He, X.; Lam, W. H.; Yam, V. W. *Chem Commun.* **2011**, *47*, 8778. (d) Sahana, A.; Banerjee, A.; Das, S.; Lohar, S.; Karak, D.; Sarkar, B.; Mukhopadhyay, S. K.; Mukherjee, A. K.; Das, D. *Org. Biomol. Chem.* **2011**, *9*, 5523. (e) Banerjee, A.; Sahana, A.; Das, S.; Lohar, S.; Guha, S.; Sarkar, B.; Mukhopadhyay, S. K.; Mukherjee, A. K.; Das, D. *Analyst* **2012**, *137*, 2166. (f) Karak, D.; Lohar, S.; Sahana, A.; Guha, S.; Banerjee, A.; Das, D. *Anal Methods* **2012**, *4*, 1906. (g) Karak, D.; Lohar, S.; Banerjee, A.; Sahana, A.; Hauli, I.; Mukhopadhyay, S. K.; Matalobos, J. S.; Das, D. *RSC Adv.* **2012**, *2*, 12447. (h) Sahana, A.; Banerjee, A.; Lohar, S.; Das, S.; Hauli, I.; Mukhopadhyay, S. K.; Matalobos, J. S.; Das, D. *Inorg. Chim. Acta* **2012**, *12*, 012 DOI: org/10.1016/j.ica.

(9) (a) Xu, Z.; Xiao, Y.; Qian, X.; Cui, J.; Cui, D. *Org. Lett.* **2005**, *7*, 889. (b) Wang, J. B.; Qian, X. F.; Cui, J. N. *J. Org. Chem.* **2006**, *71*, 4308.

(10) (a) Gunnlaugsson, T.; Davis, A. P.; O'Brien, J. E.; Glynn, M. *Org. Lett.* **2002**, *4*, 2449. (b) Vance, D. H.; Czarnik, A. W. *J. Am. Chem. Soc.* **1994**, *116*, 9397. (c) Kim, S. K.; Yoon, J. *Chem. Commun.* **2002**, 770.

(11) (a) Lim, N. C.; Schuster, J. V.; Porto, M. C.; Tanudra, M. A.; Yao, L.; Freake, H. C.; Bruckner, C. *Inorg. Chem.* **2005**, *44*, 2018. (b) Guha, S.; Lohar, S.; Banerjee, A.; Sahana, A.; Chaterjee, A.; Mukherjee, S. K.; Matalobos, J. S.; Das, D. *Talanta* **2012**, *91*, 18. (c) Das, S.; Sahana, A.; Banerjee, A.; Lohar, S.; Guha, S.; Matalobos, J. S.; Das, D. *Anal. Methods* **2012**, *4*, 2254.

(12) (a) Beer, P. D. *Acc. Chem. Res.* **1998**, *31*, 71. (b) Kim, M. J.; Konduri, R.; Ye, H.; MacDonnell, F. M.; Puntoriero, F.; Serroni, S.; Campagna, S.; Holder, T.; Kinsel, G.; Rajeshwar, K. *Inorg. Chem.* **2002**, *41*, 2471.

(13) (a) Nishizawa, S.; Kato, Y.; Teramae, N. *J. Am. Chem. Soc.* **1999**, *121*, 9463. (b) Wu, J.-S.; Zhou, J.-H.; Wang, P.-F.; Zhang, X.-H.; Wu, S.- K. *Org. Lett.* **2005**, *7*, 2133. (c) Schazmann, B.; Alhashimy, N.; Diamond, D. *J. Am. Chem. Soc.* **2006**, *128*, 8607. (d) Banerjee, A.; Sahana, A.; Guha, S.; Lohar, S.; Hauli, I.; Mukhopadhyay, S. K.; Matalobos, J. S.; Das, D. *Inorg. Chem.* **2012**, *51*, 5699. (e) Sahana, A.; Banerjee, A.; Lohar, S.; Guha, S.; Das, S.; Mukhopadhyay, S. K.; Das, D. *Analyst* **2012**, *137*, 3910.

(14) Wu, J.-S.; Liu, W.-M.; Zhuang, X.-Q.; Wang, F.; Wang, P.-F.; Tao, S.-L.; Zhang, X.-H.; Wu, S.-K.; Lee, S.-T. *Org. Lett.* **2007**, *9*, 33.

(15) (a) Sahana, A.; Banerjee, A.; Guha, S.; Lohar, S.; Chattopadhyay, A.; Mukhopadhyay, S. K.; Das, D. *Analyst* **2012**, *137*, 1544. (b) Lohar, S.; Sahana, A.; Banerjee, A.; Banik, A.; Mukhopadhyay, S. K.; Matalobos, J. S.; Das, D. *Anal. Chem.* **2013**, *85*, 1778.

(16) Peng, X.; Wu, Y.; Fan, J.; Tian, M.; Han, K. *J. Org. Chem.* **2005**, *70*, 10524.

(17) Das, S.; Guha, S.; Banerjee, A.; Lohar, S.; Sahana, A.; Das, D. *Org. Biomol. Chem.* **2011**, *9*, 7097.

(18) (a) Serin, J. M.; Brousmiche, D. W.; Frechet, J. M. J. *J. Am. Chem. Soc.* **2002**, *124*, 11848. (b) Albers, A. E.; Okreglak, V. S.; Chang, C. J. *J. Am. Chem. Soc.* **2006**, *128*, 9640. (c) Lee, S. H.; Kim, S. K.; Bok, J. H.; Lee, S. H.; Yoon, J.; Lee, K.; Kim, J. S. *Tetrahedron Lett.* **2005**, *46*, 8163. (d) Dichtel, W. R.; Serin, J. M.; Edder, C.; Frechet, J. M. J.; Matuszewski, M.; Tan, L.-S.; Ohulchanskyy, T. Y.; Prasad, P. N. *J. Am. Chem. Soc.* **2004**, *126*, 538. (e) Suresh, M.; Mishra, S.; Mishra, S. K.; Suresh, E.; Mandal, A. K.; Shrivastav, A.; Das, A. *Org. Lett.* **2009**, *11*, 2740. (f) Mahato, P.; Saha, S.; Suresh, E.; Liddo, R. D.; Parnigotto, P. P.; Conconi, M. T.; Kesharwani, M. K.; Ganguly, B.; Das, A. *Inorg. Chem.* **2012**, *51*, 1769. (g) Sreenath, K.; Allen, J.; Davidson, R. M. W.; Zhu, L. *Chem. Commun.* **2011**, *47*, 11730. (h) Wandell, R. J.; Younes, A. H.; Zhu, L. *New J. Chem.* **2010**, *34*, 2176. (i) Lohar, S.; Banerjee, A.; Sahana, A.; Banik, A.; Mukhopadhyay, S. K.; Das, D. *Anal Methods* **2013**, *5*, 442.

(19) (a) Ji, H.-F.; Brown, G. M.; Dabestani, R. *Chem. Commun.* **1999**, 609. (b) Leray, I.; O'Reilly, F.; Habib Jiwan, J.-L.; Soumillion, J.-Ph.; Valeur, B. *Chem. Commun.* **1999**, 795. (c) Leray, I.; Lefevre, J.-P.; Delouis, J.-F.; Delaire, J.; Valeur, B. *Chem.—Eur. J.* **2001**, *7*, 4590.

(20) Kim, H. N.; Lee, W. M. H.; Kim, W. H. J.; Kim, J. S.; Yoon, J. *Chem. Soc. Rev.* **2008**, *37*, 1465.

(21) Chen, X.; Pradhan, T.; Wang, F.; Kim, J. S.; Yoon, J. *Chem. Rev.* **2012**, *112*, 1910.

(22) Wu, J. S.; Hwang, I.-C.; Kim, K. S.; Kim, J. S. *Org. Lett.* **2007**, *9*, 907.

(23) Denton, D. A.; Suschitzky, H. *J. Chem. Soc.* **1963**, 4741.

(24) As per a learned reviewers advice we examined emission studies upon excitation at 475 nm (isosbestic point). However, we observed that the emission intensity is less than that of any other excitation wavelength other than 460 nm. However, if we excite at 475 nm, the emission peak due to the CHEF process (λ_{Em}, 509 nm) will merge to the shoulder due to excitation.

(25) This was not a cooperative binding model. With increasing concentration of Al(III), fluorescence intensity was increased and after a certain concentration of Al(III) emission intensity was saturated. Hence, sigmoidal nature was observed. Similar evidence was found in the literature: (a) Yang, X.; Guo, Y.; Strongin, R. M. *Angew. Chem., Int. Ed.* **2011**, *50*, 10690. (b) Roy, P.; Dhara, K.; Manassero, M.; Ratha, J.; Banerjee, P. *Inorg. Chem.* **2007**, *46*, 6405.

(26) Benesi, H. A.; Hildebrand, J. H. *J. Am. Chem. Soc.* **1949**, *71*, 2703.

(27) Best, Q. A.; Xu, R.; McCarroll, M. E.; Wang, L.; Dyer, D. J. *Org. Lett.* **2010**, *12*, 3219.